Time-to-Event Analysis of Paclitaxel-Associated Peripheral Neuropathy in Advanced Non–Small-Cell Lung Cancer Highlighting Key Influential Treatment/Patient Factors[S]

Francis W. Ojara, Andrea Henrich, Nicolas Frances, Wilhelm Huisinga, Niklas Hartung, Markus Joerger, and Charlotte Kloft

Department of Clinical Pharmacy and Biochemistry, Institute of Pharmacy, Freie Universitaet Berlin, Germany (F.W.O., A.H., C.K.); Graduate Research Training Program PharMetrX, Germany (F.W.O., A.H.); Department of Translational Modeling and Simulation, Roche Pharma Research and Early Development, Roche Innovation Center Basel, F. Hoffmann-La Roche Ltd., Basel, Switzerland (N.F.), Institute of Mathematics, University of Potsdam, Potsdam, Germany (N.H, W.H.); and Department of Oncology and Hematology, Cantonal Hospital, St. Gallen, Switzerland (M.J.)

ABSTRACT

Paclitaxel-associated peripheral neuropathy (PN), a major dose-limiting toxicity, significantly impacts patients' quality of life/treatment outcome. Evaluation of risk factors often ignores time of PN onset, precluding the impact of time-dependent factors, e.g., drug exposure, needed to comprehensively characterize PN. We employed parametric time-to-event (TTE) analysis to describe the time course of risk of first occurrence of clinically relevant PN grades ≥ 2 (PN2+, $n = 105$, common terminology criteria v4.0) and associated patient/treatment characteristics, leveraging data from 365 patients (1454 cycles) receiving paclitaxel every 3 weeks (plus carboplatin AUC = 6 or cisplatin 80 mg/m^2) for ≤ 6 cycles. Paclitaxel was intravenously administered (3 hours) as standard 200-mg/m^2 doses ($n = 182$) or as pharmacokinetic-guided dosing ($n = 183$). A cycle-varying hazard TTE model linking surge in hazard of PN2+ to paclitaxel administration [PN2+ proportions (i.e., cases per 1000 patients), 1st day, cycle 1: 4.87 of 1000; cycle 6: 7.36 of 1000] and linear decline across cycle (last day, cycle 1: 1.64 of 1000; cycle 6: 2.48 of 1000) adequately characterized the time-varying hazard of PN2+. From joint covariate evaluation, PN2+ proportions (1st day, cycle 1) increased by 1.00 per 1000 with 5-μmol·h/l higher paclitaxel exposure per cycle (AUC between the start and end of a cycle, most relevant covariate), 0.429 per 1000 with 5-year higher age, 1.31 per 1000 (smokers vs. nonsmokers), and decreased by 0.670 per 1000 (females vs. males). Compared to 200 mg/m^2 dosing every 3 weeks, model-predicted cumulative risk of PN2+ was significantly higher (42%) with 80 mg/m^2 weekly dosing but reduced by 11% with 175 mg/m^2 dosing every 3 weeks. The established TTE modeling framework enables quantification and comparison of patient's cumulative risks of PN2+ for different clinically relevant paclitaxel dosing schedules, sparing patients PN2+ to improve paclitaxel therapy.

SIGNIFICANCE STATEMENT

Characterization of risk factors of paclitaxel-associated peripheral neuropathy (PN) typically involves time-independent comparison of PN odds in patient subpopulations, concealing the impact of time-dependent factors, e.g., changing paclitaxel exposure, required to comprehensively characterize PN. We developed a parametric time-to-event model describing the time course in risk of clinically relevant paclitaxel-associated PN, identifying the highest risk in older male smokers with higher paclitaxel area under the plasma concentration-time curve between the start and end of a cycle. The developed framework enabled quantification of patient's risk of PN for clinically relevant paclitaxel dosing schedules, facilitating future dosing decisions.

Introduction

Peripheral neuropathy (PN) is a major cumulative, often irreversible, dose-limiting toxicity of paclitaxel with significant impact on patients' quality of life and may influence treatment outcome (Stubblefield et al., 2009). Over 20% of patients receiving standard paclitaxel dosing (175–200 mg/m^2, every 3 weeks) against non–small-cell lung cancer (NSCLC) experience clinically relevant PN (Joerger et al., 2016; Zhang et al., 2019). The currently accepted mechanism of paclitaxel-associated PN is through microtubule hyperstabilization, distorting the physiologic cycle of microtubule depolymerization and repolymerization and subsequently interfering with axonal growth, intracellular transport, and the structural integrity of neurons (Mielke et al., 2005; Gornstein and Schwarz, 2017). Paclitaxel-associated PN typically manifests with sensory symptoms, such as pain, paresthesia, dysesthesia, and numbness, primarily in the hands and feet, beginning

as early as 24–72 hours after administration of paclitaxel (Scripture et al., 2006; Boyette-Davis et al., 2013).

The risk of PN has been shown to increase with higher paclitaxel doses by comparing proportions of PN in patients receiving different paclitaxel doses (Green et al., 2005; Seidman et al., 2008) and higher systemic exposure, i.e., time of paclitaxel plasma concentration above 0.05 μM ($T_{C>0.05\ \mu M}$) and area under the concentration-time curve based on Kaplan-Meier analysis and logistic regression analysis (Mielke et al., 2005; Kraff et al., 2015). Duloxetine, a serotonin and norepinephrine reuptake inhibitor, is currently the only recommended treatment option for chemotherapy-induced PN symptoms (Hershman et al., 2014). However, up to 44% of the patients with paclitaxel-induced PN treated with duloxetine experience no relief (Otake et al., 2015), further emphasizing the limited treatment options.

Chemotherapy-induced PN is commonly measured using the National Cancer Institute-Common Terminology Criteria for Adverse Events (NCI-CTCAE) (https://ctep.cancer.gov). Symptoms of PN are graded in order of increasing severity from grades 0 (normal) to 4 (severe) or 5 (death). NCI-CTCAE PN grades ≥2 are considered clinically relevant, as the inflicted patient may require anticancer treatment delay or dose reductions (Park et al., 2017). To identify factors associated with increased risk of PN, the odds of occurrence of PN have been compared for different patient characteristics, including age- or treatment-related factors, such as paclitaxel exposure (Abraham et al., 2014; Kraff et al., 2015; Tanabe et al., 2017). These statistical analyses, however, ignore the influence of the time of onset of PN in describing the risk of PN and potentially conceal the underlying time-related pathophysiological or pharmacological processes, e.g., change in drug exposure over time, required to accurately characterize the occurrence of PN.

Time-to-event analysis (TTE) (Holford, 2013) provides a framework to integrate the impact of time of occurrence of PN while describing the occurrence of PN. In parametric TTE analysis, the time course in probability of PN is described using parameters of a TTE model. Prior knowledge of biologic and pharmacological processes associated with the occurrence of PN can be integrated in the model, hence providing mechanistically plausible and more accurate description of observed PN data. Parametric TTE models can further be used to simulate and predict the risk of events such as PN at specific time points for patients with specific covariate characteristics or dosing regimens (Lu et al., 2017; Svensson et al., 2018).

This work aimed to 1) describe the time course in risk of first occurrence of clinically relevant paclitaxel-associated PN using parametric TTE analysis; 2) evaluate the impact of paclitaxel exposure and relevant patient characteristics on the risk of clinically relevant PN; and 3) generate inference on the risk of clinically relevant PN for different paclitaxel dosing schedules to manage the risk of PN.

Methods

Demographic and Clinical Data. We analyzed clinical data from the CEPAC-TDM study, an open-label, randomized, phase III, multicenter study (clinicaltrials.gov identifier NCT01326767) (Joerger et al., 2016). Briefly, 365 patients with newly diagnosed advanced NSCLC received paclitaxel (3-hour intravenous infusion) plus carboplatin (target AUC = 6 mg·min/ml) or cisplatin (80 mg/m²) every 3 weeks for a maximum of six cycles. In the conventional, body surface area (BSA)-guided dosing arm, 182 patients (734 treatment cycles) received the standard paclitaxel dose of 200 mg/m², whereas in the experimental pharmacokinetic (PK)-guided dosing arm, 183 patients (720 treatment cycles) received PK-guided dosing of paclitaxel according to an algorithm based on paclitaxel exposure ($T_{C>0.05\ \mu M}$) from the previous cycle (Joerger et al., 2012). PK sampling was performed only in the PK-guided dosing arm, and $T_{C>0.05\ \mu M}$ was determined by post hoc estimation based on a paclitaxel PK model (Joerger et al., 2012). Median patient age was 64 years (range 41–78), and the proportions of females and current smokers were 33% and 37%, respectively. A detailed summary of the dosing algorithm and patient demographic and clinical characteristics has been published (Joerger et al., 2016). PN symptoms, severity, date of onset, and date of resolution were documented during study visits and graded according to NCI-CTCAE version 4.0 (https://ctep.cancer.gov).

Time-to-Event Model of Paclitaxel-Associated PN. Based on clinical judgment and literature (Park et al., 2017), PN data were dichotomized, with grade 1 categorized as clinically nonrelevant and grades ≥2 (PN2+) as clinically relevant. The first occurrence of PN2+ (incidence) within each patient was considered an event. Parametric time-to-event analysis was employed to describe the risk of PN2+ over time. In this setting, the actual time of first occurrence of PN2+ in an individual, t, was regarded as the value of a random variable, T. A hazard-based approach was used in which the distribution of T was specified through a parametric hazard function, h(t), obtained from the probability that a patient experienced first occurrence of PN2+ at time t. Based on h(t), the probability density function (pdf) of T can be derived, as well as the so-called survivor function [S(t)], which described the probability that an individual had not experienced the event before a given time t. Whenever a patient experienced an incidence of PN2+, the likelihood of the event at that time was calculated using the pdf of T, whereas if a patient never experienced PN2+, the survivor function corresponding to the final day of the last treatment cycle (censoring time) was calculated. The mathematical formulas linking h(t), S(t), and the pdf of T at time t are given as follows:

$$h(t) = \lim_{\delta t \to 0} \left\{ \frac{P(t \leq T < t + \delta t)}{\delta t} \right\} \quad (1)$$

$$S(t) = \exp\left(- \int_0^t h(u).du \right) \quad (2)$$

$$pdf(t) = S(t) \times h(t), \quad (3)$$

in which u is a variable for integration by substitution and standard notation for integration.

Different baseline hazard functions (constant, Weibull, and Gompertz) were investigated for their ability to describe the risk of first occurrence of PN2+ over time. All these functions describe a monotonic change in hazard over time. Given the knowledge on PN pathophysiology, i.e., substantial damage of the neurons 1–3 days after exposure to clinically relevant concentrations of paclitaxel (Gornstein and

---

ABBREVIATIONS: AUC area under the plasma concentration-time curve AUC_{cycle}, area under the plasma concentration-time curve between the start and end of a cycle; BSA, body surface area; CEPAC-TDM, Central European Society of Anticancer Drug Research Study of Paclitaxel Therapeutic Drug Monitoring; CI, confidence interval; CIPN, chemotherapy-induced PN; *F*, hazard surge scale factor; FCM, full covariate model; LRT, likelihood ratio test; NCI-CTCAE, National Cancer Institute-Common Terminology Criteria for Adverse Events; NSCLC, non–small-cell lung cancer; OFV, objective function value; PK, pharmacokinetic; PN, peripheral neuropathy; PN2+, peripheral neuropathy grade ≥2; $T_{C>0.01\ \mu M,\ 0.05\ \mu M,\ 0.1\ \mu M}$, time of paclitaxel plasma concentrations above thresholds of 0.01, 0.05, and 0.1 μM, respectively; TTE, time-to-event.

Schwarz, 2017), and observations in the CEPAC-TDM study, i.e., a higher proportion of patients experiencing PN2+ within the first few days after paclitaxel administration, we considered in addition a "cycle-varying hazard model" to allow for a cycle-specific change in hazard over time. In this model, a surge in hazard was linked to the administration of paclitaxel and estimated as a hazard surge term F. In this analysis, F was estimated by scaling a unit hazard introduced into the hazard compartment at the time of paclitaxel administration (Supplemental Fig. 1). Across a cycle, from the first to the last day, the hazard declined following a first-order process described by the rate constant K. Equation 4 and 5 below show the cycle-varying hazard model:

$$h(t_{Dose}) = h_{Previous} + F; \quad \text{at the cycle start,} \quad (4)$$

$$\frac{dh(t)}{dt} = -K.h(t) \quad \text{within cycle,} \quad (5)$$

in which $h(t_{Dose})$ and $h_{Previous}$ (both in day^{-1}) are the hazards of first occurrence of PN2+ at the beginning of a cycle (cycle day 1) and the end of the previous cycle, respectively (for cycle 1, $h_{Previous} = 0$); $h(t)$ (in day^{-1}) is the hazard of first occurrence of PN2+ at any cycle time t; F is the hazard surge term describing the increase in hazard of first occurrence of PN2+ at the start of a cycle, and K is the first-order hazard decay rate constant describing the decline in hazard of first occurrence of PN2+ over time within each cycle.

Impact of Covariates on Hazard of First Occurrence of PN2+. Paclitaxel PK data were only available in the PK-guided dosing arm; however, we aimed to evaluate the impact of paclitaxel PK on PN for the entire data set. As such, individual patient paclitaxel exposure metrics, i.e., time of plasma concentrations above thresholds, 0.01, 0.05, and 0.1 μM ($T_{C>0.01 \ \mu M}$, $T_{C>0.05 \ \mu M}$, and $T_{C>0.1 \ \mu M}$, respectively), and area under the plasma concentration-time curve between the start and end of a cycle (AUC_{cycle}) were derived by imputation (single and multiple) based on a PK model developed from the PK-guided dosing arm data (Henrich et al., 2017) and individual patient data (Supplemental Data). The imputation strategy was validated by comparing distributions of imputed and estimated exposure in the PK-guided dosing arm, both at individual and population levels.

Covariate analysis was performed in two steps: first, covariates were univariately evaluated with respect to F and K (based on paclitaxel exposure from single imputation) to independently determine the paclitaxel exposure metric most predictive of PN2+. Parameter-covariate relations were evaluated using the linear, proportional, and exponential models. Secondly, paclitaxel exposure, age, sex, and smoking status were jointly evaluated in a full covariate model (FCM) (Gastonguay, 2011) based on their known mechanistic pharmacological link to peripheral neuropathy. Age-related changes in nerve fibers, such as axonal atrophy, and electrophysiological changes, such as impaired nerve regeneration after injury, have been described (Verdú et al., 2000). Estrogen-mediated increase in proinflammatory cytokines and testosterone-mediated production of anti-inflammatory cytokines are linked to stronger immune response and higher sensitivity to neuropathic pain in females compared with males (Rosen et al., 2017). Smoking was found to impair functional recovery subsequent to peripheral nerve injury (Rinker et al., 2011). These covariates were also significantly associated with peripheral neuropathy in the clinical setting (Kawakami et al., 2012; de Graan et al., 2013; Kanbayashi et al., 2013). The final FCM parameters were derived after multiple imputation (50 replicates) of paclitaxel exposure (Johansson and Karlsson 2013; Svensson et al., 2018). The dependence of covariate effects of paclitaxel exposure, age, sex, and smoking status on treatment arm (BSA-guided or PK-guided dosing) was assessed by estimating the FCM parameters with and without treatment arm as a covariate. Subsequently, based on the estimated FCM parameters, 250 virtual clinical trials were simulated for a standard paclitaxel dosing schedule, varying the level of a specific covariate while keeping other covariates at reference value, and cumulative proportions of PN2+ were computed at the end of treatment.

Time-to-Event Model Evaluation. To compare the different baseline hazard models and evaluate the FCM, Kaplan-Meier visual predictive checks were used: 250 data sets were generated by simulation from the developed models, followed by graphical comparison of the simulated and observed data. In univariate covariate analysis, the likelihood ratio test (LRT) was used to assess statistical significance of covariates. For any two nested models, e.g., the baseline TTE model (with no covariates) and a covariate model, a change in objective function value of ≥3.84 points as numeric quality criterion for covariate inclusion showed statistical significance of the covariate effect, corresponding to an asymptotic type 1 error of $\alpha = 0.05$ (χ^2 distribution with one degree of freedom, corresponding to one additional model parameter).

Risk of PN2+ with Different Paclitaxel Dosing Schedules. Exploiting the developed TTE full covariate model, simulations were performed to evaluate the risk of first occurrence of PN2+ in three clinically relevant paclitaxel dosing schedules for NSCLC (summarized in Table 1). A virtual population of 1000 patients with NSCLC was generated by sampling with replacement from the distribution of patient characteristics in the CEPAC-TDM data base: sex and smoking status were sampled empirically (i.e., without consideration for the distribution of other patient characteristics), whereas age was sampled based on the distribution within the respective sex. All three dosing schedules were administered to each patient, one at a time, and typical paclitaxel PK exposure was derived using the paclitaxel PK model (Henrich et al., 2017). Parameters (250 sets) of the FCM without treatment arm effect were sampled from their uncertainty distributions, and for each set, a clinical trial was simulated based on the virtual populations. Hence, model parameter uncertainty and randomness of the time-to-event model were the two levels of variability included during the simulations. As outcome, 1) the simulated proportion of patients who experienced PN2+ was compared between the different dosing schedules across time during treatment, and 2) risk ratios between the different dosing schedules were computed based on simulated proportions of PN2+ at the end of treatment of each trial.

Software. Data set preparation and statistical evaluation were performed in R 3.4.3 (https://www.r-project.org), and TTE analysis was performed with the first-order method in NONMEM 7.3.0 with assistance of PsN 4.2.0 (Lindbom et al., 2005) and Pirana 2.9.4 (Keizer et al., 2011).

Results

Exploratory PN Data Analysis. In total, 105 patients (28.8%) experienced a first occurrence of PN2+ during any treatment cycle. Generally, a higher number of events were observed in the first few days subsequent to paclitaxel treatment administration (cycle start), with the numbers gradually declining across the cycle in all observed cycles (Fig. 1, solid line). The number of events recorded on day 1 of a cycle increased across cycles; no event was recorded on day 1 of the first cycle. No specific trend in proportion of incidence of PN2+ across treatment cycles was apparent; however, cycle 1 had the lowest proportion of PN2+ (5.6%), with cycle 4 having the highest proportion of PN2+ (14.6%).

TABLE 1
Selected clinically relevant paclitaxel dosing schedules

Schedule	Dosing Frequency
200 mg/m² every 3 weeks	Day 1 of a 21-day cycle, 6 cycles
175 mg/m² every 3 weeks	Day 1 of a 21-day cycle, 6 cycles
80 mg/m² once every week	Days 1, 8, 15 of a 28-day cycle, 6 cycles
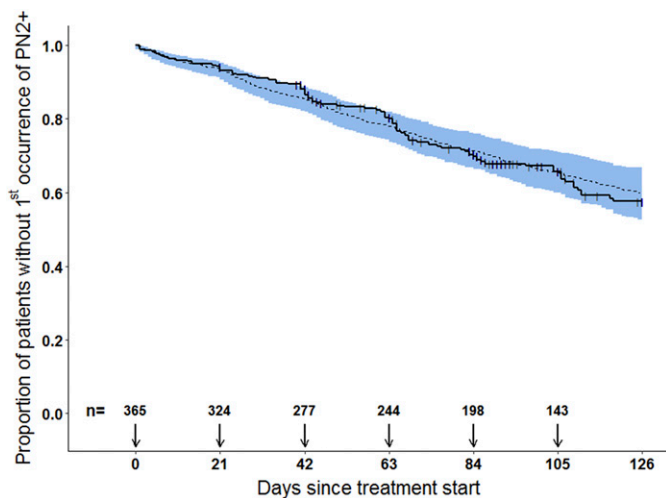
Fig. 1. Kaplan-Meier visual predictive check for the cycle-varying hazard baseline time-to-event model showing observed and model prediction of first occurrence of PN2+. Proportion of patients without first occurrence of PN2+ is plotted across time, with observations censored at the last protocol treatment time. Solid line: observed data (vertical lines: censor times due to dropout from various reasons); dashed line: median model-predicted profile, 90% CI (blue shade); *n* is the number of patients at specific observation times; arrows: day of planned paclitaxel administration as specified in the study protocol.

Of the 260 patients who did not experience PN2+, 75 received six cycles of treatment (meaning they did not drop out but were censored at the end of the study period), whereas the remaining 185 patients were considered dropouts (censored at dropout) with regard to PN2+ analysis. The reasons for dropout included tumor progression (43.0%), patient death (13.0%), and among others, cessation of treatment at physician's discretion, withdrawal of consent, and intolerable non-neurologic toxicities. Therefore, drop-outs were assumed random with regard to PN2+ and not explicitly accounted for in developing this time-to-event model of peripheral neuropathy.

Time-to-Event Model of Paclitaxel-Associated PN2+. Based on the LRT, no statistically significant difference in model fit was found between the constant, Weibull, and Gompertz hazard models (change in OFV < 3.84 points between the three models but 24.4 higher than cycle-varying hazard model, Supplemental Table 1). However, as the cycle-varying hazard and constant hazard models were not nested, these models were compared using visual predictive checks (Supplemental Fig. 2, A–D), rather than the LRT. The cycle-varying hazard model best characterized the observed profile of first occurrence of PN2+ across time. In contrast to the constant, Weibull, and Gompertz hazard models (Supplemental Fig. 3, A–C), the cycle-varying hazard model (Supplemental Fig. 3D) described an increase in hazard of PN2+ at cycle start, followed by the gradual decrease within the cycle. As such, the cycle-varying hazard model was adopted for subsequent analyses.

Impact of Covariates on the Hazard of first Occurrence of PN2+. Paclitaxel exposure from single imputation closely matched the exposure estimated based on paclitaxel PK, and both fell largely within the interquartile range of paclitaxel exposure from multiple imputation by comparison at both individual and population levels (Supplemental Figs. 4 and 5), demonstrating reliability of the imputation procedure. Hence, individual imputed paclitaxel exposure was adopted in both the BSA-guided and PK-guided dosing arms for further covariate evaluation. Generally, paclitaxel exposure (paclitaxel AUC_{cycle}, $T_{C>0.01\ \mu M}$, $T_{C>0.05\ \mu M}$, and $T_{C>0.1\ \mu M}$) was not constant, mainly as a result of dose adaptations in the PK-guided dosing arm, but gradually declined across treatment cycles with increase in variability between patients (AUC_{cycle} and $T_{C>0.05\ \mu M}$ shown in Fig. 2).

Paclitaxel AUC_{cycle}, $T_{C>0.01\ \mu M}$, $T_{C>0.05\ \mu M}$, and $T_{C>0.1\ \mu M}$ all had a statistically significant impact on the hazard of first occurrence of PN2+ (Table 2) from univariate analysis, whereas trends of increase in hazard of PN2+ were observed with older patients, males compared with females, and current smokers compared with current nonsmokers. Higher paclitaxel exposure was associated with a higher surge in hazard or a lower rate of decline in hazard across time when evaluated against F or K, respectively, resulting in a higher risk of PN2+ within a cycle. Based on the LRT, paclitaxel AUC_{cycle} on F was associated with the greatest improvement in model fit compared to the base model with no covariates (16.1-point drop in OFV, Table 2). The impact of paclitaxel AUC_{cycle} on PN2+ was less significant when evaluated with respect to K (reduction in OFV of 12.1). Joint evaluation of the impact of paclitaxel AUC_{cycle} with respect to F and K did not further improve model fit compared with F alone, i.e., change in OFV of 17.3, although it reduced the precision of parameter estimates. This could be attributed to the strong correlation between F and K. Furthermore, the condition number for the model with the impact of paclitaxel AUC_{cycle} on F was 84.3 excluding ill conditioning. As such, we retained the impact of paclitaxel AUC_{cycle} only on F for subsequent full covariate modeling.

Joint Evaluation of the Impact of Covariates Using a Full Covariate Model. Based on mechanistic pharmacologic plausibility of covariates on PN and prior clinical knowledge (Kawakami et al., 2012; de Graan et al., 2013; Kanbayashi et al., 2013), age, sex, and smoking status were included for joint evaluation in an FCM. The relationship between covariates and the hazard surge term (F) in the FCM was parameterized as shown in eqs. 6 and 7 for the models without and with treatment arm as covariate, respectively:

$$F = TVF \cdot \exp(E_{AUC} \cdot (AUC_{cycle} - AUC_{(cycle,med)})$$
$$\times \cdot \exp(E_{Age} \cdot (Age - Age_{med})) \cdot (E_{Sex})^{Sex} \cdot (E_{Smok})^{Smoker} \quad (6)$$

$$F = TVF \cdot \exp(E_{ARM} \cdot ARM) \cdot \exp(E_{AUC} \cdot (AUC_{cycle} - AUC_{(cycle,med)}))$$
$$\exp(E_{Age} \cdot (Age - Age_{med})) \cdot (E_{Sex})^{Sex} \cdot (E_{Smok})^{Smoker}, \quad (7)$$

in which TVF is the typical value of F for a male (sex = 0, sex = 1 for females) current nonsmoker (smoker = 0, smoker = 1 for current smokers) of median age (Age_{med} = 64 years) and median paclitaxel AUC_{cycle} [$AUC_{(cycle,\ med)}$]; ARM (BSA-guided dosing = 0, PK-guided dosing = 1) is covariate for treatment arm; E_{AUC}, E_{Age}, E_{Sex}, E_{Smok}, and E_{Arm} are covariate effect coefficients for paclitaxel AUC_{cycle}, age, sex, smoking status, and treatment arm, respectively.

Based on parameter estimates of the FCM with no treatment arm effect (eq. 6), an F of 0.00487 day^{-1} (Table 3) was estimated as the hazard on the first day of treatment of a typical patient population [males, current nonsmokers with median age (64 years), and paclitaxel AUC_{cycle}], which translated into on average 4.87 in 1000 patients experiencing PN2+. This hazard declined with a first-order rate constant
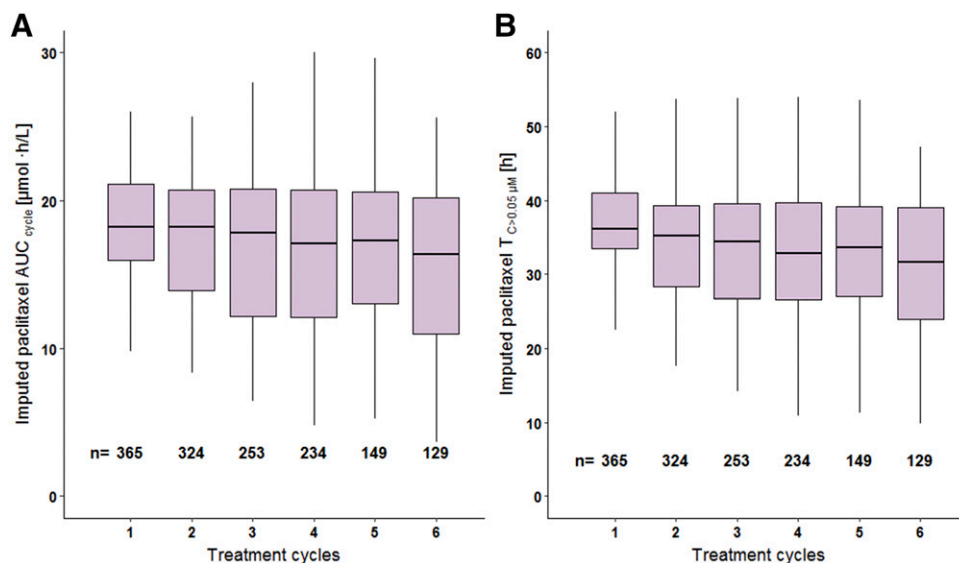
Fig. 2. Distribution of imputed paclitaxel exposure across treatment cycles for the BSA-guided and PK-guided dosing arms combined. Panel A: AUC_{cycle}; panel B: time of plasma concentrations above the threshold of 0.05 μM ($T_{C>0.05\ \mu M}$). Boxes: interquartile range (IQR), including median; whiskers (vertical lines): range from box hinge, values within $\pm 1.5 \bullet IQR$; n is the number of patients receiving paclitaxel for a given cycle.

($K = 0.0518$ day^{-1}) to 0.00164 day^{-1} on day 21 (last day of a cycle 1), i.e., 1.64 in 1000 patients experiencing PN2+. For cycle 6, the hazards on days 1 and 21 were 0.00733 and 0.00247, respectively, translating into 7.33 in 1000 and 2.47 in 1000 patients experiencing PN2+ on days 1 and 21, respectively. The estimated FCM parameters adequately predicted the observed time-course of of first occurrence of PN2+ (Supplemental Fig. 8).

Covariate impact assessment (by varying a specific covariate while keeping the rest at typical values) revealed a 20% increase in F (1.00 per 1000 increase in proportions of PN2+) and 43% increase in F (2.10 per 1000 increase in proportions of PN2+) for a 5 and 10 μmol·h/l increase in paclitaxel AUC_{cycle}, respectively; a 9% increase in F (0.429 per 1000 increase in proportions of PN2+) and 18.5% increase in F (0.900 per 1000 increase in proportions of PN2+) for a 5- and 10-year increase in age, respectively; and a 27% higher F (1.31 per 1000 increase in proportions of PN2+) in smokers compared with nonsmokers and a 14% lower F (0.670 per 1000 decrease in proportions of PN2+) in females compared with males. Of note, for the continuous covariates AUC_{cycle} and age due to the exponential function of the relation on F, a higher exposure and higher age led to a more pronounced effect on F, i.e., increase in hazard of first occurrence of PN2+ at the start of a cycle. Visualization of covariate impact in terms of proportions of patients experiencing PN2+ across time on treatment is shown in Supplemental Fig. 6. Based on the 250 virtual clinical trial simulations, the estimated percentage

increase in risk of PN2+, comparing the 97.5th and 2.5th percentiles of covariate distributions, was 22.0% and 62.0% for paclitaxel AUC_{cycle} with and without treatment arm effect, respectively, in contrast to 39.0% and 44.0% for age with and without treatment arm effect, respectively (Fig. 3), revealing a much stronger dependence of the covariate effect of paclitaxel AUC_{cycle} on treatment arm compared with that of age on treatment arm.

Risk of PN2+ with Different Paclitaxel Dosing Schedules. The percentage cumulative risk of PN2+ at the end of treatment with 200 mg/m^2 dosing every 3 weeks was 44.2% (90% CI: 32.4%–54.8%) and 64.1% (90% CI: 45.0%–78.3%) for the 80 mg/m^2 weekly dosing schedule, i.e., the 80 mg/m^2 weekly dosing schedule was associated with significantly higher cumulative risk of PN2+ compared with dosing 200 mg/m^2 every 3 weeks with a risk ratio of 42.0% (90% CI: 9.00%–90.0%) (Table 4) after accounting for randomness of the time-to-event model and parameter uncertainty. Although dosing 200 mg/m^2 every 3 weeks was associated with a more profound increase in risk of PN2+ with each paclitaxel administration compared to 80 mg/m^2 weekly dosing, the higher dosing frequency in weekly dosing led to a gradual increase in risk of PN2+ with higher minimum risk of PN2+ after each paclitaxel administration, hence a higher overall cumulative risk of PN2+ (Supplemental Fig. 78). However, a large overlap in proportions of patients experiencing PN2+ was predicted across time between the two dosing schedules (Fig. 4A). For the 175 compared with 200 mg/m^2

TABLE 2
Parameter estimates (relative S.E., %) of the cycle-varying hazard base model and covariate models implementing different imputed paclitaxel pharmacokinetics exposure metrics

Parameter	Base Model: No Covariate	Covariate Model with $T_{C>0.01\ \mu M}$	Covariate Model with $T_{C>0.05\ \mu M}$	Covariate Model with $T_{C>0.1\ \mu M}$	Covariate Model with AUC_{cycle}
OFV	1344.323	1337.249	1334.563	1332.735	1328.224
F, day^{-1}	0.00568 (35)	0.00500 (40)	0.00480 (41)	0.00460 (41)	0.00460 (42)
K, day^{-1}	0.0568 (42)	0.0504 (49)	0.0480 (52)	0.0477 (51)	0.0448 (55)
E_{COV}, covariate unit^{-1}	n.a	0.0329 (43)	0.0456 (38)	0.0652 (33)	0.0989 (29)

E_{COV}, covariate effect parameter describing change in F with a unit change in paclitaxel exposure relative to the median exposure; K, first-order hazard decay rate constant.
n.a: not applicable

TABLE 3
Pooled parameter estimates [(relative S.E., %), (95% confidence intervals)] of the cycle-varying hazard full covariate model after multiple imputation
Covariate-parameter relations were implemented using an exponential model for paclitaxel AUC_{cycle}, age, and treatment arm (BSA-guided dosing = 0, PK-guided dosing = 1) and a power model for sex (male = 0, female = 1) and smoking status (current nonsmokers = 0, current smokers = 1). The 95% CI of each parameter was derived from S.E. values of estimated parameters by transformation of the variance-covariance matrices. n.a: not applicable

Parameter	Parameter Description	Model with No Arm Effect	Model with Arm Effect
F, day^{-1}	Hazard surge scale factor	0.00487 (42.6), (0.000852, 0.00880)	0.00659 (43.5), (0.000974, 0.0122)
K, day^{-1}	Hazard decay rate constant	0.0518 (47.9), (0.00311, 0.100)	0.0531 (47.2), (0.00486, 0.103)
E_{Arm}	Treatment arm effect on F	n.a	−0.621 (41.6), (−1.13, −0.114)
E_{AUC}, 1/(μmol·h/l)	Paclitaxel AUC_{cycle} effect on F	0.0359 (51.1), (0.0000320, 0.0718)	0.00154 (151.5), (−0.0308, 0.0611)
E_{Age}, y^{-1}	Age effect on F	0.0169 (84.1), (−0.0107, 0.0445)	0.0154 (91.4), (−0.0122, 0.0429)
E_{Sex}	Sex effect on F	0.864 (22.2), (0.488, 1.23)	0.841 (22.0), (0.478, 1.20)
E_{Smok}	Smoking status effect on F	1.27 (20.4), (0.761, 1.78)	1.33 (20.2), (0.804, 1.85)

dosing every 3 weeks, an 11.0% lower risk of PN2+ (90% CI: 20.5% decrease, 1.00% increase) was predicted (Fig. 4B; Table 4), though not statistically significant.

Discussion

A parametric cycle-varying hazard TTE model based on knowledge of pathophysiology and trends of occurrence of clinically relevant peripheral neuropathy (PN2+) was developed to characterize the time course of the risk of first occurrence of PN2+ in paclitaxel-treated patients with advanced NSCLC: the risk of PN2+ significantly increased with higher paclitaxel AUC_{cycle}, and the most vulnerable population was identified as the older, male, and current smokers from joint evaluation of covariate impacts. The established model enables improved prediction of an individual patient's risk of PN2+ with different clinically relevant paclitaxel dosing schedules for dose selection during treatment.

TTE analysis offers marked improvements over common approaches used for analyzing PN data: traditionally, odds of PN are compared across different patient subpopulations to ascertain associated risk factors (Scripture et al., 2006; Kanbayashi et al., 2013; Tanabe et al., 2017). These approaches only account for the occurrence of the event without consideration for the time of occurrence and as such conceal knowledge on time-dependent pathophysiological or pharmacological processes required to adequately characterize and predict the occurrence of PN. In the CEPAC-TDM study, a Kaplan-Meier–based nonparametric TTE analysis was used to compare the risk of PN between BSA-guided and PK-guided dosing strategies (Joerger et al., 2016). As an extension, parametric TTE analysis was adopted in this work, which allowed 1) basing on prior knowledge on the pathophysiology of PN to better describe the baseline hazard of first occurrence of PN2+; 2) a mechanistic evaluation of the impact of nonstratified time-varying covariates, e.g., paclitaxel AUC_{cycle}; and 3) simulation of the occurrence of PN for different paclitaxel exposure levels (dosing regimens) and patient characteristics based on the developed parametric hazard function (TTE model).

The cycle-varying hazard model best described the observed PN2+ data: a surge in incidence of PN2+ at cycle start was linked to the administration of paclitaxel, with the magnitude estimated using the hazard surge term (F). The gradual decline in hazard across time within a cycle was best described as a first-order process, using the hazard decline rate constant (K). Variability in parameters F and K between different patients was linked to differences in patient-specific covariate characteristics. This model structure is supported by in vitro data showing that adult dorsal root ganglion neurons, the cell type inflicted by paclitaxel-associated neurotoxicity, undergo substantial damage 1–3 days after exposure to clinically relevant concentrations of paclitaxel (Gornstein and Schwarz, 2017). This was also consistent with observations from the CEPAC-TDM study, i.e., a higher proportion of patients experienced PN2+ within the first few days after paclitaxel administration.

The effect of paclitaxel exposure could be estimated separately on F and K; however, this was not possible on both F and K simultaneously in the same model. Paclitaxel exposure had a stronger effect on F compared with K, with AUC_{cycle} showing a stronger effect than $T_{C>0.01\ \mu M}$, $T_{C>0.05\ \mu M}$, and $T_{C>0.1\ \mu M}$. Previous studies also showed a statistically significant increase in the risk of PN with higher AUC and $T_{C>0.05\ \mu M}$ (Mielke et al., 2005; de Graan et al., 2013; Zhang et al., 2016). Unlike these studies, we accounted for cycle-specific changes in exposure, allowing the hazard in an individual to change across cycles, resulting in a more accurate description of the risk of PN2+ across time with changing paclitaxel exposure. The increase in risk of PN2+ with higher paclitaxel exposure
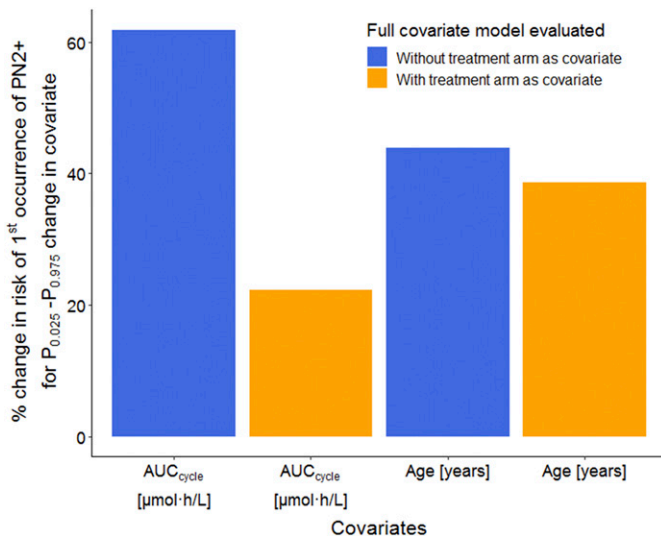
Fig. 3. Increase in risk of first occurrence of PN2+ with change in covariate level. Proportions of first occurrence of PN2+ were simulated at 2.5th percentile ($P_{0.025}$) and 97.5th percentile ($P_{0.975}$) covariate levels using the cycle-varying hazard full covariate models with (orange) and without (blue) treatment arm as a covariate and percentage change in risk of PN2+ calculated. In each case, the covariate of interest was set to the specified percentile while maintaining the remaining covariates at their reference values.

TABLE 4
Comparison of risk of first occurrence of PN2+ (90% confidence intervals) between different clinically relevant paclitaxel dosing schedules

Schedule	Percentage of PN2+	Risk Ratio	
		175 mg/m^2 Every 3 Weeks: 200 mg/m^2 Every 3 Weeks	80 mg/m^2 Once Every Week: 200 mg/m^2 Every 3 Weeks
200 mg/m^2 every 3 weeks	44.2 (32.4, 54.8)	n.a	n.a
175 mg/m^2 every 3 weeks	39.6 (29.4, 49.3)	0.891 (0.795, 1.01)	n.a
80 mg/m^2 once every week	64.1 (45.0, 78.3)	n.a	1.42 (1.09, 1.90)

n.a: not applicable

suggests the need for prophylactic management or closer monitoring of symptoms of PN2+ early on within cycles, especially in subpopulations at higher risk of PN2+ (elderly, male, current smokers), to enable early treatment, e.g., with duloxetine (Otake et al., 2015).

Inclusion of treatment arm effect (BSA-guided vs. PK-guided) as a covariate on F was associated with a 65% reduction in the covariate effect of paclitaxel AUC_{cycle}. This trend was expected, since protocol dose adaptations in the CEPAC-TDM study led to lower paclitaxel AUC_{cycle} in the PK-guided compared to the BSA-guided dosing arm; hence, the observed relationship between treatment arm and PN2+ is attributed to the difference in paclitaxel AUC_{cycle} between the two dosing arms. Treatment arm only partly reduced the covariate effect of paclitaxel AUC_{cycle}, meaning that paclitaxel AUC_{cycle} was a stronger predictor of PN2+ compared with treatment arm.

Our findings suggest a higher cumulative risk of PN2+ with 80 mg/m^2 weekly dosing compared to 200 mg/m^2 paclitaxel dosing every 3 weeks. Weekly dosing was associated with a lower surge in risk of PN2+ for a single paclitaxel administration; however, a higher cumulative risk of PN2+ was predicted because of the higher dosing frequency. Previous comparisons of neuropathy risk between weekly dosing and paclitaxel dosing every 3 weeks yielded mixed findings (Green et al., 2005; Schuette et al., 2006; Belani et al., 2008; Seidman et al., 2008; Sparano et al., 2008; Fountzilas et al., 2009). Lower paclitaxel $T_{C>0.01 \text{ }\mu M}$ with weekly dosing compared with dosing every 3 weeks was associated with reduced toxicity, especially hematologic toxicities (Marchetti et al., 2002). For dosing every 3 weeks, the cumulative risk of PN2+ increased with higher paclitaxel doses, i.e., higher in 200 mg/m^2 compared to 175 mg/m^2. Ultimately, our results suggest a reduction in risk of PN2+ with paclitaxel dose reduction rather than dose fractionation (same overall paclitaxel dose administered multiple times within a cycle). Given similar efficacy (progression-free and overall survival) in the dose range of $175–200 \text{ mg/m}^2$ (Joerger et al., 2016), the lower risk of PN2+ with 175 mg/m^2 paclitaxel dosing every 3 weeks suggests an improved therapeutic benefit compared with 200 mg/m^2 paclitaxel dosing every 3 weeks.

Alternative time-to-event models that describe a symmetric phase of increase and decrease in hazard of events at predefined times have been employed before for characterizing different events (Plan et al., 2011; Tarning et al., 2014). However, this model structure inadequately described observed PN2+ profiles in this study. Proportions of observed PN2+ peaked a few days after paclitaxel administration and gradually declined over time across the cycle, a profile not consistent with the symmetric model. Alternatively, the hazard of first occurrence of PN2+ could be described using an indirect response model (Upton and Mould, 2014). The paclitaxel concentration-time profiles may be used to drive either the rate of development of the hazard or inhibit the rate of decline of the hazard. The differences in time scale of measurement of paclitaxel concentration and PN2+ events (i.e., hours vs. days) would require fixing PN2+ incidence to a specific clock time, hence introducing a bias in the concentration-PN2+ relationship; as such, we opted for the cycle-varying hazard model and evaluated the time course of incidence of PN2+ on a time scale of days.

In previous characterization of the time course of chemotherapy-induced PN (CIPN) during paclitaxel treatment, Mehrotra et al. (2017) used a kinetic-pharmacodynamic indirect response model. CIPN scores (0–16) were derived from PN grades from the Functional Assessment of Cancer Therapy/Gynecologic Oncology Group-Neurotoxicity grading system and were
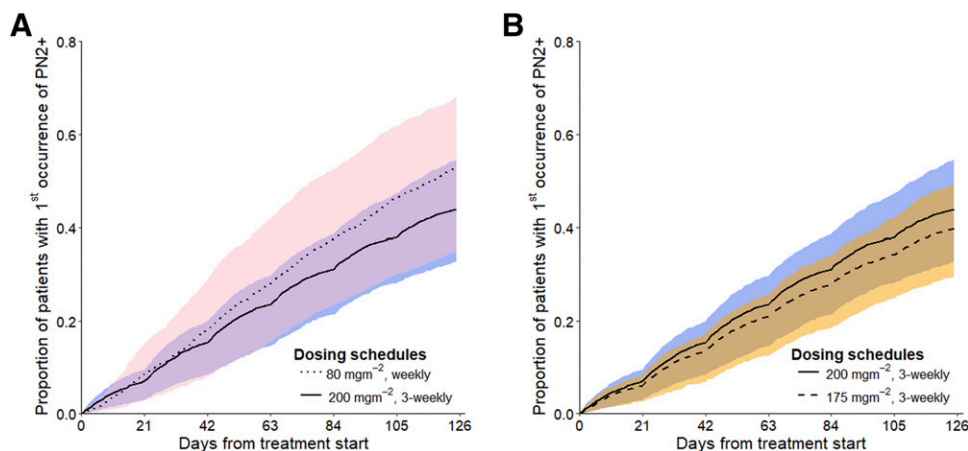
Fig. 4. Cumulative risk of first occurrence of PN2+ across time on treatment. (Panel A) Weekly dosing of 80 mg/m^2 vs. 200 mg/m^2 dosing every 3 weeks; (panel B) 200 mg/m^2 dosing every 3 weeks vs. 175 mg/m^2 dosing every 3 weeks. Shades represent 90% CI of simulated proportion of patients experiencing first occurrence of PN2+ across time on treatment. Pink: 80 mg/m^2 weekly dosing; blue: 200 mg/m^2 dosing every 3 weeks; orange: 175 mg/m^2 dosing every 3 weeks.

treated as a continuous variable; a score of 4.00 could represent mild experience of each of the four items (score = 1). Our data base contained NCI-CTCAE PN grades 1–3 (only three categories) and hence cannot be modeled as a continuous variable. Our model-predicted proportion of PN2+ after six cycles of weekly 80 mg/m^2 paclitaxel dosing was 64.1% (90% CI: 45.0%–78.3%), whereas the kinetic-pharmacodynamic model-predicted CIPN scores ≥4.00 was 45.6% for a patient with BSA of 1.87 m^2.

As a possible limitation, our model did not account for the impact of the potentially neurotoxic coadministered platinum drugs. Cisplatin is more neurotoxic than carboplatin, with neuropathy incidences of 28%–100% compared with 6%–42% with carboplatin (Stubblefield et al., 2009). Our data base contained only PK for paclitaxel. In univariate covariate evaluation with respect to F or K, platinum drug type had no statistically significant impact, with covariate impacts estimated with unreliably wide confidence intervals. The most probable reason was the low proportion of patients, i.e., 17% (63 out of 365) cotreated with cisplatin in cycle 1, 14% (9 out of 63) of whom changed to carboplatin in later cycles. This introduces a bias in discriminating the covariate impact of platinum drug type. Although only paclitaxel impact was evaluated, the underlying hazard may partly be attributed to coadministered drugs, suggesting an overestimated impact of paclitaxel exposure in this clinically used drug combination treatment protocol in NSCLC.

In conclusion, we successfully developed a parametric cycle-varying hazard TTE model characterizing the time course of risk of first occurrence of clinically relevant paclitaxel-associated PN. Parametrically describing the baseline hazard of PN2+ enabled basing on mechanistic pharmacologic knowledge, e.g., time-dependent change in risk of PN2+ with change in paclitaxel exposure, to improve the characterization of observed PN2+ and enable better prediction of future incidences. FCM evaluation of covariate effects enabled better characterization of the impact of clinically relevant risk factors of PN2+, revealing older, male, and current smokers with high paclitaxel AUC$_{cycle}$ as the highest-risk subpopulation and offering opportunity for prophylactic intervention or closer monitoring of symptoms for timely treatment. Model-based comparisons suggested that reduction in risk of PN2+ was attainable through dose reduction rather than dose fractionation. The model enables prediction and comparison of individual patient's risks of PN2+ for different clinically relevant paclitaxel dosing schedules, facilitating dose selection to spare patients the disabling PN2+ and improve paclitaxel combination therapy.

Authorship Contributions

Participated in research design: Ojara, Henrich, Huisinga, Hartung, Joerger, Kloft.

Performed data analysis: Ojara.

Wrote or contributed to writing of the manuscript: Ojara, Henrich, Frances, Huisinga, Hartung, Joerger, Kloft.

References

Abraham JE, Guo Q, Dorling L, Tyrer J, Ingle S, Hardy R, Vallier AL, Hiller L, Burns R, Jones L, et al. (2014) Replication of genetic polymorphisms reported to be associated with taxane-related sensory neuropathy in patients with early breast cancer treated with paclitaxel. *Clin Cancer Res* 20:2466–2475.

Belani CP, Ramalingam S, Perry MC, LaRocca RV, Rinaldi D, Gable PS, and Tester WJ (2008) Randomized, phase III study of weekly paclitaxel in combination with carboplatin versus standard every-3-weeks administration of carboplatin and paclitaxel for patients with previously untreated advanced non-small-cell lung cancer. *J Clin Oncol* 26:468–473.

Boyette-Davis JA, Cata JP, Driver LC, Novy DM, Bruel BM, Mooring DL, Wendelschafer-Crabb G, Kennedy WR, and Dougherty PM (2013) Persistent chemoneuropathy in patients receiving the plant alkaloids paclitaxel and vincristine. *Cancer Chemother Pharmacol* 71:619–626.

de Graan AJ, Elens L, Sprowl JA, Sparreboom A, Friberg LE, van der Holt B, de Raaf PJ, de Bruijn P, Engels FK, Eskens FA, et al. (2013) CYP3A4*22 genotype and systemic exposure affect paclitaxel-induced neurotoxicity. *Clin Cancer Res* 19:3316–3324.

Fountzilas G, Dafni U, Dimopoulos MA, Koutras A, Skarlos D, Papakostas P, Gogas H, Bafaloukos D, Kalogera-Fountzila A, Samantas E, et al. (2009) A randomized phase III study comparing three anthracycline-free taxane-based regimens, as first line chemotherapy, in metastatic breast cancer: a Hellenic Cooperative Oncology Group study. *Breast Cancer Res Treat* 115:87–99.

Gastonguay MR(2011) Full covariate models as an alternative to methods relying on statistical significance for inferences about covariate effects: a review of methodology and 42 case studies, in *Population Approach Group Europe (PAGE)*; 2011 Jun 7–10; Athens, Greece. PAGE 20: 2229 [www.page-meeting.org/default.asp?abstract=2229].

Gornstein EL and Schwarz TL (2017) Neurotoxic mechanisms of paclitaxel are local to the distal axon and independent of transport defects. *Exp Neurol* 288:153–166.

Green MC, Buzdar AU, Smith T, Ibrahim NK, Valero V, Rosales MF, Cristofanilli M, Booser DJ, Pusztai L, Rivera E, et al. (2005) Weekly paclitaxel improves pathologic complete remission in operable breast cancer when compared with paclitaxel once every 3 weeks. *J Clin Oncol* 23:5983–5992.

Henrich A, Joerger M, Kraff S, Jaehde U, Huisinga W, Kloft C, and Parra-Guillen ZP (2017) Semimechanistic bone marrow exhaustion pharmacokinetic/pharmacodynamic model for chemotherapy-Induced cumulative neutropenia. *J Pharmacol Exp Ther* 362:347–358.

Hershman DL, Lacchetti C, Dworkin RH, Lavoie Smith EM, Bleeker J, Cavaletti G, Chauhan C, Gavin P, Lavino A, Lustberg MB, et al.; American Society of Clinical Oncology (2014) Prevention and management of chemotherapy-induced peripheral neuropathy in survivors of adult cancers: American Society of Clinical Oncology clinical practice guideline. *J Clin Oncol* 32:1941–1967.

Holford N (2013) A time to event tutorial for pharmacometricians. *CPT Pharmacometrics Syst Pharmacol* 2:e43.

Joerger M, Kraff S, Huitema ADR, Feiss G, Moritz B, Schellens JH, Beijnen JH, and Jaehde U (2012) Evaluation of a pharmacology-driven dosing algorithm of 3-weekly paclitaxel using therapeutic drug monitoring: a pharmacokinetic-pharmacodynamic simulation study. *Clin Pharmacokinet* 51:607–617.

Joerger M, von Pawel J, Kraff S, Fischer JR, Eberhardt W, Gauler TC, Mueller L, Reinmuth N, Reck M, Kimmich M, et al. (2016) Open-label, randomized study of individualized, pharmacokinetically (PK)-guided dosing of paclitaxel combined with carboplatin or cisplatin in patients with advanced non-small-cell lung cancer (NSCLC). *Ann Oncol* 27:1895–1902.

Johansson ÅM and Karlsson MO (2013) Multiple imputation of missing covariates in NONMEM and evaluation of the method's sensitivity to η-shrinkage. *AAPS J* 15:1035–1042.

Kanbayashi Y, Hosokawa T, Kitawaki J, and Taguchi T (2013) Statistical identification of predictors for paclitaxel-induced peripheral neuropathy in patients with breast or gynaecological cancer. *Anticancer Res* 33:1153–1156.

Kawakami K, Tunoda T, Takiguchi T, Shibata K, Ohtani T, Kizu J, Nishio M, Horai T, Hama T, and Taguchi K (2012) Factors exacerbating peripheral neuropathy induced by paclitaxel plus carboplatin in non-small cell lung cancer. *Oncol Res* 20:179–185.

Keizer RJ, van Benten M, Beijnen JH, Schellens JH, and Huitema AD (2011) Piraña and PCluster: a modeling environment and cluster infrastructure for NONMEM. *Comput Methods Programs Biomed* 101:72–79.

Kraff S, Nieuweboer AJ, Mathijssen RH, Baty F, de Graan AJ, van Schaik RH, Jaehde U, and Joerger M (2015) Pharmacokinetically based dosing of weekly paclitaxel to reduce drug-related neurotoxicity based on a single sample strategy. *Cancer Chemother Pharmacol* 75:975–983.

Lindbom L, Pihlgren P, and Jonsson EN (2005) PsN-Toolkit--a collection of computer intensive statistical methods for non-linear mixed effect modeling using NONMEM [published correction appears in *Comput Methods Programs Biomed* (2005) 80:277]. *Comput Methods Programs Biomed* 79:241–257.

Lu D, Gillespie WR, Girish S, Agarwal P, Li C, Hirata J, Chu YW, Kagedal M, Leon L, Maiya V, et al. (2017) Time-to-event analysis of polatuzumab vedotin-induced peripheral neuropathy to assist in the comparison of clinical dosing regimens. *CPT Pharmacometrics Syst Pharmacol* 6:401–408.

Marchetti P, Urien S, Cappellini GA, Ronzino G, and Ficorella C (2002) Weekly administration of paclitaxel: theoretical and clinical basis. *Crit Rev Oncol Hematol* 44 (Suppl):S3–S13.

Mehrotra S, Sharma MR, Gray E, Wu K, Barry WT, Hudis C, Winer EP, Lyss AP, Toppmeyer DL, Moreno-Aspitia A, et al. (2017) Kinetic-Pharmacodynamic model of chemotherapy-induced peripheral neuropathy in patients with metastatic breast cancer treated with paclitaxel, nab-paclitaxel, or ixabepilone: CALGB 40502 (Alliance). *AAPS J* 19:1411–1423.

Mielke S, Sparreboom A, Steinberg SM, Gelderblom H, Unger C, Behringer D, and Mross K (2005) Association of Paclitaxel pharmacokinetics with the development of peripheral neuropathy in patients with advanced cancer. *Clin Cancer Res* 11:4843–4850.

Otake A, Yoshino K, Ueda Y, Sawada K, Mabuchi S, Kimura T, Kobayashi E, Isobe A, Egawa-Takata T, Matsuzaki S, et al. (2015) Usefulness of duloxetine

for Paclitaxel-induced peripheral neuropathy treatment in gynecological cancer patients. *Anticancer Res* **35**:359–363.

Park SB, Kwok JB, Asher R, Lee CK, Beale P, Selle F, and Friedlander M (2017) Clinical and genetic predictors of paclitaxel neurotoxicity based on patient- versus clinician-reported incidence and severity of neurotoxicity in the ICON7 trial. *Ann Oncol* **28**:2733–2740.

Plan EL, Ma G, Någård M, Jensen J, and Karlsson MO (2011) Transient lower esophageal sphincter relaxation pharmacokinetic-pharmacodynamic modeling: count model and repeated time-to-event model. *J Pharmacol Exp Ther* **339**:878–885.

Rinker B, Fink BF, Barry NG, Fife JA, Milan ME, Stoker AR, and Nelson PT (2011) The effect of cigarette smoking on functional recovery following peripheral nerve ischemia/reperfusion injury. *Microsurgery* **31**:59–65.

Rosen S, Ham B, and Mogil JS (2017) Sex differences in neuroimmunity and pain. *J Neurosci Res* **95**:500–508.

Schuette W, Blankenburg T, Guschall W, Dittrich I, Schroeder M, Schweisfurth H, Chemaissani A, Schumann C, Dickgreber N, Appel T, et al. (2006) Multicenter randomized trial for stage IIIB/IV non-small-cell lung cancer using every-3-week versus weekly paclitaxel/carboplatin. *Clin Lung Cancer* **7**:338–343.

Scripture CD, Figg WD, and Sparreboom A (2006) Peripheral neuropathy induced by paclitaxel: recent insights and future perspectives. *Curr Neuropharmacol* **4**: 165–172.

Seidman AD, Berry D, Cirrincione C, Harris L, Muss H, Marcom PK, Gipson G, Burstein H, Lake D, Shapiro CL, et al. (2008) Randomized phase III trial of weekly compared with every-3-weeks paclitaxel for metastatic breast cancer, with trastuzumab for all HER-2 overexpressors and random assignment to trastuzumab or not in HER-2 nonoverexpressors: final results of Cancer and Leukemia Group B protocol 9840. *J Clin Oncol* **26**:1642–1649.

Sparano JA, Wang M, Martino S, Jones V, Perez EA, Saphner T, Wolff AC, Sledge GW Jr, Wood WC, and Davidson NE (2008) Weekly paclitaxel in the adjuvant treatment of breast cancer. *N Engl J Med* **358**:1663–1671.

Stubblefield MD, Burstein HJ, Burton AW, Custodio CM, Deng GE, Ho M, Junck L, Morris GS, Paice JA, Tummala S, et al. (2009) NCCN task force report: management of neuropathy in cancer. *J Natl Compr Canc Netw* **7** (Suppl 5):S1–S26, quiz S27–S28.

Svensson EM, Svensson RJ, Te Brake LHM, Boeree MJ, Heinrich N, Konsten S, Churchyard G, Dawson R, Diacon AH, Kibiki GS, et al. (2018) The potential for treatment shortening with higher rifampicin doses: relating drug exposure to treatment response in patients with pulmonary tuberculosis. *Clin Infect Dis* **67**: 34–41.

Tanabe Y, Shimizu C, Hamada A, Hashimoto K, Ikeda K, Nishizawa D, Hasegawa J, Shimomura A, Ozaki Y, Tamura N, et al. (2017) Paclitaxel-induced sensory peripheral neuropathy is associated with an ABCB1 single nucleotide polymorphism and older age in Japanese. *Cancer Chemother Pharmacol* **79**: 1179–1186.

Tarning J, Thana P, Phyo AP, Lwin KM, Hanpithakpong W, Ashley EA, Day NP, Nosten F, and White NJ (2014) Population pharmacokinetics and antimalarial pharmacodynamics of piperaquine in patients with plasmodium vivax malaria in Thailand. *CPT Pharmacometrics Syst Pharmacol* **3**:e132.

Upton RN and Mould DR (2014) Basic concepts in population modeling, simulation, and model-based drug development: part 3-introduction to pharmacodynamic modeling methods. *CPT Pharmacometrics Syst Pharmacol* **3**:e88.

Verdú E, Ceballos D, Vilches JJ, and Navarro X (2000) Influence of aging on peripheral nerve function and regeneration. *J Peripher Nerv Syst* **5**:191–208.

Zhang J, Zhou F, Qi H, Ni H, Hu Q, Zhou C, Li Y, Baburina I, Courtney J, and Salamone SJ (2019) Randomized study of individualized pharmacokinetically-guided dosing of paclitaxel compared with body-surface area dosing in Chinese patients with advanced non-small cell lung cancer. *Br J Clin Pharmacol* **85**: 2292–2301.

Zhang S, Sun M, Yuan Y, Wang M, She Y, Zhou L, Li C, Chen C, and Zhang S (2016) Correlation between paclitaxel Tc > 0.05 and its therapeutic efficacy and severe toxicities in ovarian cancer patients. *Cancer Transl Med* **2**:131–136.

Address correspondence to: Charlotte Kloft, Department of Clinical Pharmacy and Biochemistry, Institute of Pharmacy, Freie Universitaet Berlin., Kelchstr. 31, 12169 Berlin, Germany. E-mail: charlotte.kloft@fu-berlin.de